Accepted Manuscript

Kinetics of the electronic center annealing in Al_2O_3 crystals

V.N. Kuzovkov, E.A. Kotomin, A.I. Popov

PII: S0022-3115(17)31509-X

DOI: 10.1016/j.jnucmat.2018.02.022

Reference: NUMA 50795

To appear in: *Journal of Nuclear Materials*

Received Date: 25 October 2017

Revised Date: 14 February 2018

Accepted Date: 14 February 2018

Please cite this article as: V.N. Kuzovkov, E.A. Kotomin, A.I. Popov, Kinetics of the electronic center annealing in Al_2O_3 crystals, *Journal of Nuclear Materials* (2018), doi: 10.1016/j.jnucmat.2018.02.022.

Kinetics of the electronic center annealing in Al_2O_3 crystals

V. N. Kuzovkov[1], E. A. Kotomin[1,2], A.I. Popov[1]

[1]*Institute of Solid State Physics, Kengaraga 8, Riga LV 1063, Latvia*

[2]*Max Planck Institute for Solid State Research, Heisenbergstr. 1, Stuttgart 70569, Germany*

Abstract

The experimental annealing kinetics of the primary electronic F , F^+ centers and dimer F_2 centers observed in Al_2O_3 produced under neutron irradiation were carefully analyzed. The developed theory takes into account the interstitial ion diffusion and recombination with immobile F-type and F_2-centers, as well as mutual sequential transformation with temperature of three types of experimentally observed dimer centers which differ by net charges (0, +1, +2) with respect to the host crystalline sites. The relative initial concentrations of three types of F_2 electronic defects before annealing are obtained, along with energy barriers between their ground states as well as the relaxation energies.

Keywords: Al_2O_3; radiation defects; F centers; F_2 centers; diffusion; recombination; annealing kinetics

*Corresponding author. Tel: +371 67187480. E-mail address: kotomin@latnet.lv (E.A. Kotomin)

1. Introduction

α-Al_2O_3 (corundum, sapphire) is important radiation-resistant material with potential applications for components of diagnostic windows and breeder blankets [1–8]. The radiation-induced vacancies in oxygen sublattice produce electronic defects (color centers) with trapped one or two electrons (the F^+ and F centers, respectively) [9-12].

The F type centers in Al_2O_3 show a distinctive optical absorption: at 203 nm (6.1 eV) (F centers) and 256 nm (4.8 eV) (F^+ centers). Properties of complementary interstitial impurity atoms O_i are much less known due to absence of magnetic moment and optical absorption in a suitable energy range. It is known, however, that in most binary oxides (as well as in alkali halides) [13-15] the anion interstitials are considerably more mobile than complementary vacancies and thus the F-type center annealing at intermediate temperatures (in MgO and Al_2O_3 around 400-500 K) arises due to the recombination of *immobile* electron centers with mobile interstitials. This is supported by the fact that F center aggregation in thermochemically reduced MgO [16-18] and Al_2O_3 [1,19] (when only F centers exist) occurs at very high temperatures, typically above 1500 K. Similar picture was also observed in yttria-stabilized-zirconia (YSZ) [20] and BeO [21].

Under intensive neutron, ion or fast electron irradiation of Al_2O_3, or even high-frequency induction heating method, along with single defects, dimer F_2 electron centers are also observed [1,22-30]. Dimer F_2 centers are also found in some other oxides, including MgO, CaO and Li_2O [9,31-39].

These defects consist of two nearest oxygen vacancies trapped different number of electrons [5,6] which is confirmed in the case of Al_2O_3 by theoretical calculations [40]. Three types of F_2 centers reveal optical absorption at 302 nm (4.1 eV), 356 nm (3.5 eV) and 450 nm (2.7 eV) [1,22,23].

The study of the F- and F_2 electronic center annealing is important for prediction and control of radiation stability of oxide materials. Recently, we developed phenomenological theory describing the diffusion-controlled kinetics of the Frenkel defect annealing in ionic solids [41,42] and demonstrated how analysis of the experimental data allows us to extract two control parameters: the migration energy of the interstitial ions E_a and pre-factor $X = n_0RD_0/\beta$, where n_0 is initial defect concentration, R recombination radius, D_0 diffusion pre-exponent, and β heating rate.

In this paper, we generalized this theory, taking into account dimer F_2 centers and their mutual transformation and recombination. We have analyzed in detail available experimental kinetics of both the single *F*- and dimer F_2 type center annealing in Al_2O_3 in a wide temperature range (300-1200 K).

2. Theoretical

Our model of radiation defect annealing includes the following steps: (i) primary Frenkel defects (vacancies and interstitials, in case of Al_2O_3 these are the *F*-type centers and O_i interstitials) are produced by radiation in equal concentrations, (ii) defects migrate with the diffusion coefficients determined by the migration energies E_a and pre-exponentials D_0, (iii) The *F* centers mobile at high temperatures attract each other and form metallic colloids, (iv) the dissimilar defects recombine upon mutual approach within a critical distance *R* through the bimolecular reaction, (v) the post-irradiation annealing occurs with the linear increase of the temperature, (vi) three types of immobile dimer F_2 centers created under intensive irradiation can mutually transform $F_2(1) \rightarrow F_2(2)$, $F_2(2) \rightarrow F_2(3)$, and recombine with mobile interstitials. More mathematical details are discussed in Appendix.

As was shown [16,41,43,44], the *F* centers in thermochemically reduced (TCR) sapphire are mobile only above 1500 K. Below this temperature *F*-type center recombination and transformation in irradiated samples are controlled by much more mobile oxygen interstitials [9,41]. This is well observed, for example, in alkali halides [13, 42]. However, in TCR samples with high concentration of impurities and mobile vacancies *defect-assistant* *F* center migration and dimer formation could also occur at reduced temperatures [17,43]. Fitting our theoretical kinetics to the experimental data on the *F* center annealing, we can extract the migration energies of interstitials and the pre-exponential factors *X*, containing D_0.

3. Results

3.1. The *F* centers

We found in the literature a number of experimental studies for the electronic *F*- and F^+ center annealing in neutron irradiated sapphire, and analyzed 10 available kinetics. Six of these annealing kinetics are shown in Fig.1, whereas the kinetic parameters obtained for all 10 kinetics are summarized in Table 1. Note that these kinetics differ considerably by

experimental conditions, first of all, neutron energies and fluxes. This results in a considerable variation of the migration energies and pre-exponentials summarized in Table 1.

Table 1. The calculated migration energies of interstitial oxygen ions E_a and pre-exponential factors X for 10 kinetics from the literature (see references). The experimental and theoretical kinetics (points and full lines) for the first six cases are shown in Fig.1.

Nr.	Type	E_a (eV)	X (K^{-1})	Reference
1	F	0.79	2.1×10^{1}	[43]
2	F^+	0.89	7.0×10^{1}	[43]
3	F^+	0.40	2.3×10^{-1}	[3], Fig.4
4	F^+	0.47	1.2×10^{0}	[23], Fig.5
5	F^+	0.39	5.3×10^{-1}	[22], Fig.3
6	F^+	0.27	4.0×10^{-1}	[45], Fig.2c
7	F	0.22	3.3×10^{-2}	[45], Fig.2a
8	F	0.17	1.3×10^{-2}	[22], Fig.2
9	F	0.14	1.9×10^{-3}	[46], Fig.3
10	F^+	0.35	1.4×10^{0}	[1], Fig.12b

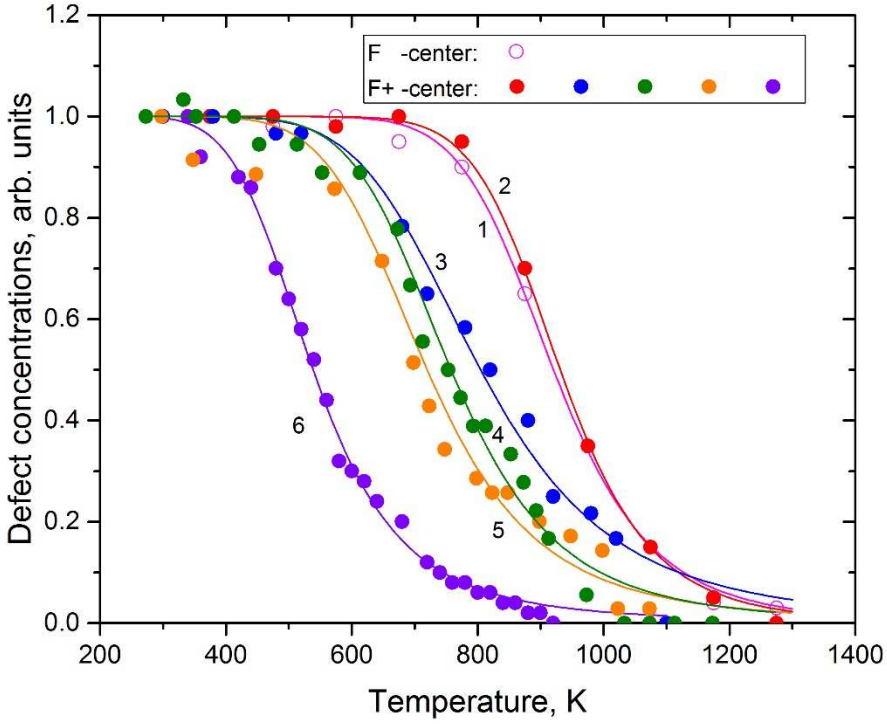

Fig.1. The kinetics of the F or F^+ center annealing for different neutron fluxes (see Table 1 for details).

We attribute a strong dependence of the E_a and X parameters to the variation in radiation defect concentrations (the irradiation flux). As one can see, decrease of the diffusion energies is accompanied by decrease, by orders of magnitude, of the pre-exponential factors. Moreover, pre-exponential factors X are typically much smaller than its simple estimate for normal diffusion in crystals (assuming $n_0 = 10^{17}$cm^{-3}, R= 10 Å, $D_0 = 10^{-3}$ cm^2 s^{-1}, β= 10 K/min, one expects the X=10^8 K^{-1}). We believe that this is result of increasing material disordering with larger and larger fluences which is supported by recent experimental [47] and theoretical [48] studies. The smallest fluxes correspond to curves 1 and 2 (the F and F^+ centers), which show the largest O_i migration energies (0.8-0.9 eV) and largest pre-factors X=20-70 K^{-1}. This migration energy is indeed close to theoretically calculated value for the *charged* interstitial ions [49], and considerably smaller than the estimate for the neutral interstitial [50]. Note that the calculated migration energy of the electronic F centers is much larger, 4.5 eV [41], therefore, these defects are immobile at the temperature range shown in Fig.1.

Second, the annealing curves for the F and F^+ centers (curves 1 and 2 in Fig.1) decay sinchronously which means that no transformation $F \rightarrow F^+$ occurs; both defects recombine independently with mobile interstitials. The difference of 0.1 eV in the obtained migration energies could serve as an accuracy estimate of our theory.

3.2. Dimer centers

In this Section, we discuss the annealing of the dimer F_2 center kinetics observed in two experimental studies [22,23]. As is seen in Fig.1, curves 4 and 5 for the F^+ centers in these experiments decay smoothly and show no peculiarities due to presence and transformation of dimer defects, due to dimer relatively small concentrations. Following original papers, Fig.2 shows the normalized annealing kinetics of the three F_2- centers from ref. [22] whereas these kinetics were not normalized in ref. [23]. (In our analysis we normalized data [23] for analysis and returned them back to original form in Fig.3). Note that this is generally believed (e.g. [22,23]) that three types of the dimer centers are created as the result of bimolecular reactions between single mobile vacancies, e.g. $F + F \rightarrow F_2$, $F + F^+ \rightarrow F_2^+$ and $F^+ + F^+ \rightarrow F_2^{2+}$. However, we understand now that the F-centers are immobile at the relevant temperatures and thus mutual transformation of the dimer centers is electronic process controlled by electrons thermal ionization from vacancies and re-trapping by other vacancies. Essentially, the F_2 type centers observed [22,23] were

created during the irradiation (e.g. as a result of overlap of tracks produced by neutrons) but not sample annealing. In parallel, the total F_2 concentration decreases, as well as that for the single defects, due to recombination with the mobile interstitials.

Let us analyze now data in Fig.2, and denote F_2 centers in the sequence of their appearance: F_2 (1) corresponds to the peak at 302 nm, F_2(2) 450 nm, F_2(3) 356 nm. As one can see, concentration of the single *F* centers monotonous decreases (see Fig. 1, curve (5)) whereas three dimer centers show very different behavior: similar but faster monotonous decay of F_2(1), a sharp F_2(2) peak in the temperature range of the F_2(1) decay, and F_2(3) peak at higher temperatures where F_2(2) centers decay.

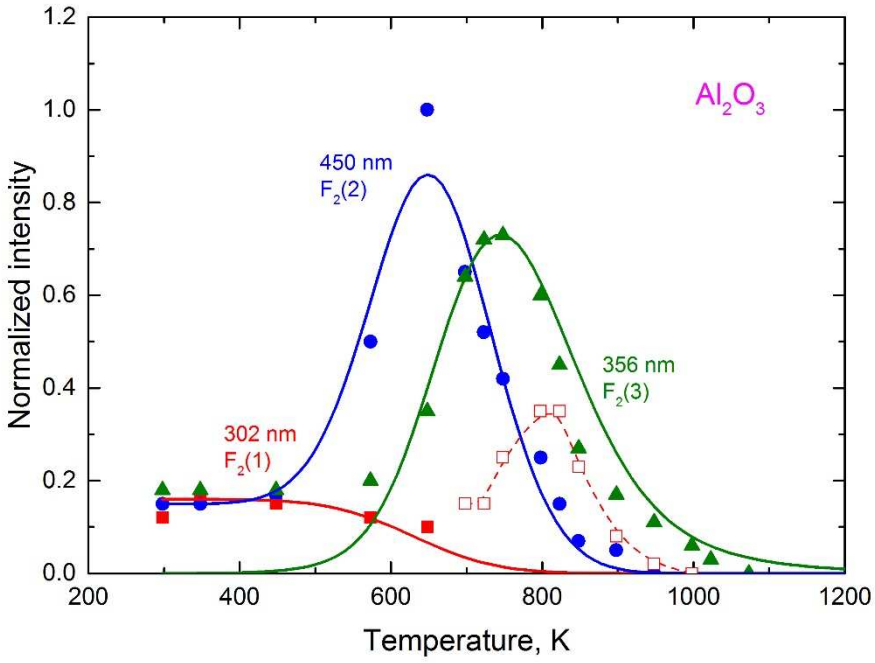

Fig.2. Experimental points from ref. [22] and their theoretical analysis (full lines). Maximum of the 450 nm band intensity was normalized to unity. Background was substracted and peaks normalized. Empty red squares very likely do not related to the F2(1) band (e.g. see discussion in Ref. [23], p.2990, for more details) and were neglected in our analysis.

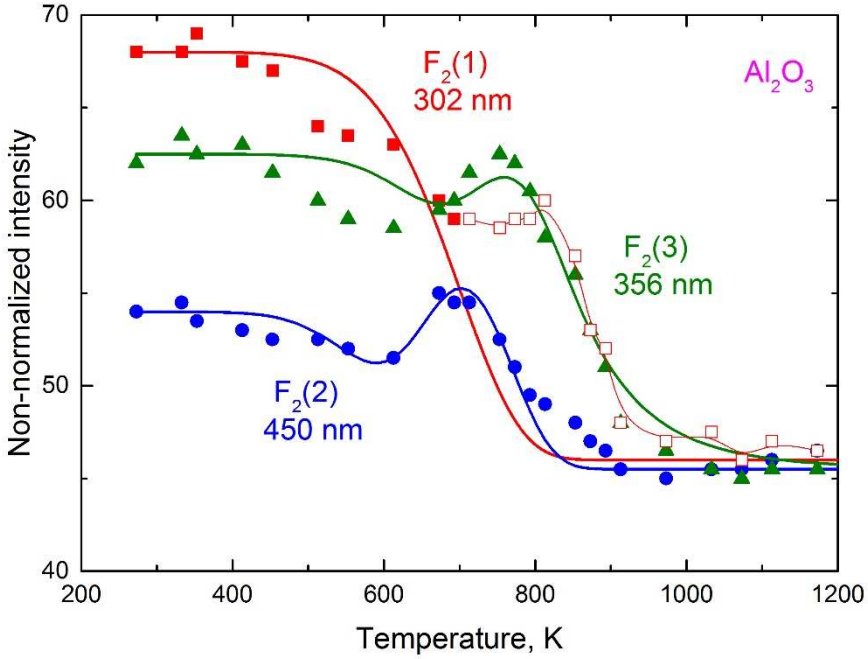

Fig.3. Non-normalized experimental points from ref.[23] and their theoretical analysis (full lines).

This supports idea of mutual transformation of three types of dimer centers. The fact that the *F* center decay is not affected by the mentioned peculiarities in the F_2 kinetics indicates at a negligible concentration of dimer centers compared to that of the *F* centers. This allows us to treat kinetics of the *F* and F_2 centers independently which greatly simplifies the problem. In particular, while considering the kinetics of dimer centers, the concentration of hole centers could be taken from solution for the kinetics for single centers. The basic equations for the dimer center kinetics are discussed in the Appendix. Here we concentrate on the basic results.

As mentioned above, the annealing kinetics of dimer centers is a combination of the two independent processes: recombination of immobile electron centers with mobile interstitials (hole centers) and mutual transformation of three types of F_2-type centers: $F_2(1) \rightarrow F_2(2)$, and $F_2(2) \rightarrow F_2(3)$. As shown in Appendix, total concentration of all dimer centers is defined by the single, *F* center decay kinetics $C(t) = n(t)/n(0)$, as $C^{\kappa}(t)$, where $\kappa = R_2/R$, R and R_2 are recombination radii for interstitials with single and dimer centers.

Three dimers could be characterized by relative concentrations (probabilities) $W_i(t)$, i=1,2,3, with the normalization $W_1(t)+ W_2(t)+ W_3(t)=1$ and initial condition $W_i(0)=w_i$. The dimer concentrations are defined as products $W_i(t)C(t)^{\kappa}$. These concentrations were rescaled in Fig.2, following data presentation in ref.[23].

The equations for probabilities (see Appendix) describe dimer center mutual transformations, $F_2(1) \rightarrow F_2(2)$ with the rate $p_1=p_1^0\exp(-E_b/k_BT)$, and then $F_2(2) \rightarrow F_2(3)$ (with the rate $p_2=p_2^0\exp(-E_c/k_BT)$). Fitting theoretical curves to the experimental ones, we have obtained the main kinetic parameters – activation energies E_b and E_c, two pre-exponents $P_1=p_1^0/\beta$ and $P_2=p_2^0/\beta$, recombination parameter κ and initial defect populations w_i.

The results are shown in Fig.2 and Fig.3 in full curves and summarized in Table 2. As one can see, a simple model describes very well a whole set of experimental data.

Table 2. The obtained parameters of mutual dimer center transformations.

Ref.	**F centers diffusion**		**F_2 center mutual transformation**						
	Activation energy	Pre-exponent	Activation enegies		Pre-exponents		Populations		
	E_a , eV	X , K^{-1}	E_b ,eV	E_c ,eV	P_1 , K^{-1}	P_2 , K^{-1}	W_1	W_2	W_3
[22]	0.39	$5.3\cdot10^{-1}$	0.46	0.32	$9.7\cdot10^{0}$	$4.3\cdot10^{0}$	0.99	0.01	0.00
[23]	0.47	$1.2\cdot10^{0}$	0.87	0.47	$9.5\cdot10^{3}$	$1.6\cdot10^{2}$	0.78	0.02	0.20

The parameter κ=2.06 [22] and 1.66 [23]

The calculated activation energies for mutual center transformations based on data [22] are similar, E_b=0.46 eV and E_c=0.32 eV and close to the Oi migration energy E_a=0.39 eV, three related pre-exponents are also close: $X=5.3\cdot10^{-1}$ K^{-1}, $P_1=9.7\cdot10^{0}$ K^{-1} and $P_2=4.3\cdot10^{0}$ K^{-1}. The parameter κ=2.06 is close to the ratio of geometric cross sections of an interstitial recombination with the single defect and di-vacancy. Lastly, the initial $F_2(1)$ dimer population is predominant, $w_1=0.992$, whereas that for $F_2(2)$ is very small, and negligible for $F_2(3)$.

The analysis of data [23] demonstrates that transformation energies are slightly larger than in ref.[22]: E_b=0.87 eV and E_c=0.47 eV, as well as O_i migration energy E_a=0.47 eV. Three related pre-exponents are also close: $X=1.2\cdot10^{0}$ K^{-1}, $P_1=9.5\cdot10^{3}$ K^{-1} and $P_2=1.6\cdot10^{2}$ K^{-1}. The parameter κ=1.66 is again close to the ratio of geometric cross sections of a single and di-vacancy. Lastly, the initial $F_2(1)$ dimer populations is

large, $w_1=0.78$, $F_2(2)$ dimer populations is very small, $w_2=0.02$, whereas population of the third dimer is intermediate, $w_3=0.20$. At any rate, $F_2(1)$ dimers again are predominant defects after irradiation and before annealing.

Temperature evolution of three types of dimer concentrations in both experiments [22,23] is shown in Figs. 4 and 5. It is well seen here that the main difference lies in the larger initial concentration of $F_2(3)$ dimers under experimental conditions of ref. [23] but qualitatively results are very similar.

It could be assumed that mutual transformation of three F_2-type centers correspond to three possible dimer charges: F_2, F_2^+ and F_2^{2+} (four, three and two trapped electrons in the di-vacancy (see Fig. 3 [51], Fig. 3 [40]) which occurs via *electronic* process -- dimers successive thermal ionization with release each time one electron, $F_2 \rightarrow F_2^+ + e$ and $F_2^+ \rightarrow F_2^{2+} + e$, respectively. This hypothesis needs further careful analysis.

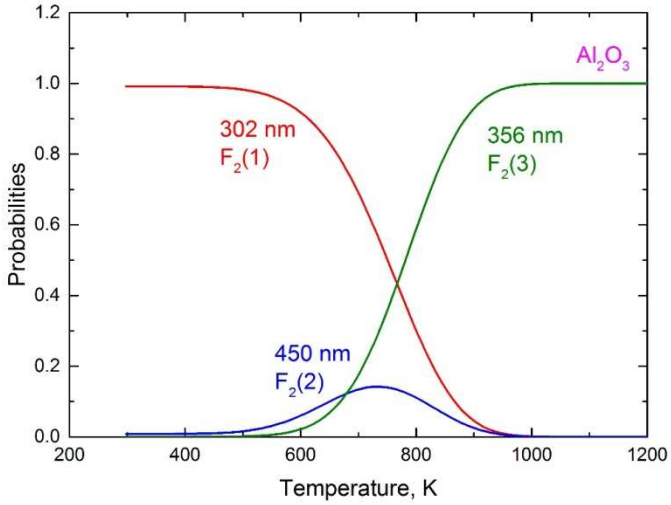

Fig.4. The calculated temperature dependence of dimer center populations [22].

Along with sequential dimer center transformations $F_2(1) \rightarrow F_2(2)$, $F_2(2) \rightarrow F_2(3)$, we considered more general processes including hypothetical reaction $F_2(1) \rightarrow F_2(3)$ and reversible reactions (with electron trapping): $F_2(3) \rightarrow F_2(2)$, $F_2(2) \rightarrow F_2(1)$. (This analysis is based on our previous experience with reversible chemical reactions [52,53]. More details are available from authors by request). The main conclusions are as follows: (i) The hypothetical process $F_2(1) \rightarrow F_2(3)$ does not occur, only sequential transformations $F_2(1) \rightarrow F_2(2)$, $F_2(2) \rightarrow F_2(3)$ take place, (ii) The rates

of above mentioned reversible processes are neglegibly small. Similar analysis shown that there is no mutual transformation of the *F* and F^+ centers.

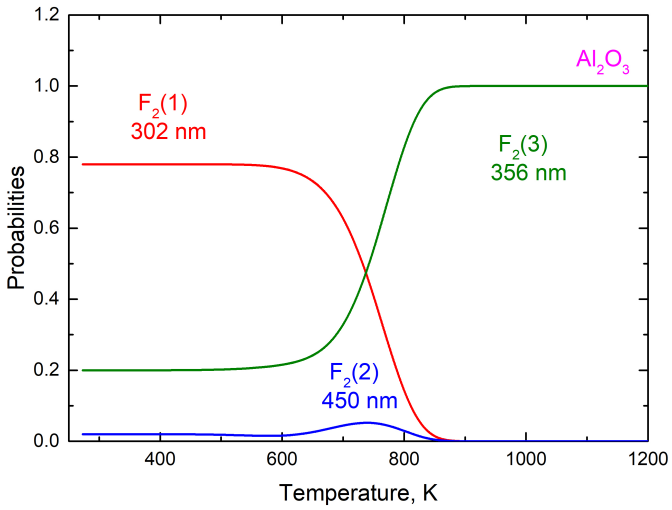

Fig.5. same as Fig.4 for data in ref.[23].

4. Conclusions

Phenomenological theory of the diffusion-controlled annealing kinetics of single and dimer electron centers in irradiated oxides was developed and applied to Al_2O_3 crystals. Theoretical analysis of the available experimental kinetics for the *F* type centers produced under neutron irradiation shows strong dependence of the migration energy and pre-exponent for oxygen interstitial ions on the radiation fluence which is ascribed to increasing material disordering [48]. The migration energy of 0.8 eV for lowest fluence (almost perfect crystal) is in a good agreement with theoretical prediction for *charged* oxygen interstitials in crystalline matrix [49].

Analysis of the kinetics of the mutual transformation of three types of dimer F_2-type centers observed under intensive neutron irradiation [22,23] allows us to extract all kinetic parameters and supports the idea that these three centers differ by the charge states (neutral, single- and double-charged defects with respect to the perfect crystal). We suggest the following center interpretation: 302 nm - F_2, 450 nm - F_2^+ , and 356 nm F_2^{2+}. Note, that determination of the defect charge states is very non-trivial problem; there is also no unique opinion in the literature also for F_2-type dimer centers [9,22,23,29,30,40,51], which needs further analysis. The general hypothesis of

different charge states and electronic processes behind their mutual transformations is supported by our similar results for three types of dimer centers observed in MgF_2 [54] and discussed in ref. [28]. It is also clearly shown here that this transformation does not involve migration of single *F*-type centers [29].

In some publications (e.g. [23]) the absorption band at 300 nm was tentatively ascribed to Al_i^+ interstitials, citing old studies, e.g. by Evans [55]. However, this hypothesis was not experimentally proved and in later review paper by Evans [56] was not considered at all, the whole defect scenario was within the framework of the concept of the *F*, *F+* and large family of different F_2 centers. In this connection situation is quite similar to MgO, where radiation-induced Mg interstitial optical absorption never was observed. Moreover, theoretical calculations [57] indicate that Al_i^+ could be stable only at very low temperature due to low barrier for back recombination, whereas $F_2(1)$ start to decay above 600 K (Fig. 4).

The *ab initio* calculations of the atomic and electronic structure of three dimer centers could give better understanding of the parameters E_b, E_c and relevant pre-exponentials, in order to discreminate between the electron thermal ionization and delocalization between different dimer centers, or their ionic restructuring and transformations.

5. Acknowledgments

Authors are greatly indebted to A. Ch. Lushchik, V. Kortov, M. Izerrouken and R.Vila for stimulating discussions. This work has been carried out within the framework of the Eurofusion Consortium and has received funding from the Euroatom research and training programme 2014-2018 under grant agreement No 633053. The views and opinions expressed herein do not necessarily reflect those of the European Commission. The calculations were performed using facilities of the Stuttgart Supercomputer Center (project DEFTD 12939).

Appendix

1. Single center annealing kinetics

Changes of the *F*-type center and interstitial (hole, *H*) concentrations are described by the bimolecular reaction

$$\frac{d\,n_F(t)}{dt} = \frac{d\,n_H(t)}{dt} = -\boldsymbol{K n_F(t) n_H(t)}\,, \qquad \text{(A1)}$$

where $n_F(t)$ and $n_H(t)$ are defect concentrations; $n_F(t) = n_H(t) = n(t)$. Our study shows that the *F*- and F^+- centers reveal the same recombination rates *K* and do not transform one to another. It is convenient to introduce the dimensionless defect concentration $C(t) = n(t)/n(0)$, *C(0)*=1. The *F* centers are immobile at temperatures 400-1200 K, whereas oxygen interstitials migrate with the diffusion coefficients $D = D_0 \exp(-E_a/k_B T)$, E_a is the activation energy. The recombination rate could be well approximated as $K = 4\pi DR$ [58], where R is recombination radius, typically of the $R \sim a_0$ (see discussion of this approximation in refs. [59-61]).

The defect concentration decay reads

$$\boldsymbol{d\left(\frac{1}{C(t)}\right) = K n_0 dt} \quad , \qquad \text{(A2)}$$

where $n_0 = n(0)$. For the linear temperature increase with the rate $\beta = \frac{d}{dt}T(t) = const$, eq. (1) becomes

$$\boldsymbol{\frac{1}{C(T)} = 1 + 4\pi X \int_{T_0}^{T} \exp\left(-\frac{E_a}{k_B T}\right) dT}\,, \qquad \text{(A3)}$$

where $X = n_0 R D_0/\beta$ is a combination of basic paramters, and $T_0 = T(0)$.

We used eq. (3) for the least square fitting to the experimental kinetics, which gives us two main kinetic parameters *X* and E_a presented in table 1.

2. Dimer center kinetics

The smooth decay of the single *F*-type center concentrations in Fig. 1 is obviously not affected by changes in the dimer center concentration shown in Figs. 2 and 3. This proves that relative concentrations of dimer centers are small compared to those of single defects and thus one could consider both kinetics independently, neglecting in particular, formation of additional *F* centers due to recombination of mobile interstitials and F_2 centers and decay of interstitial concentration due to recombination with F_2 compared with that with single electronic centers.

As discussed above, kinetics of dimer centers includes both their bimolecular recombination with mobile interstitials and mutual transformation of three types of F_2-type centers (monomolecular processes), $F_2(1) \rightarrow F_2(2)$, and $F_2(2) \rightarrow F_2(3)$. As the

result, the dimer center decay is described by the bimolecular diffusion-controlled reaction

$$\frac{d\, n_{F_2}(t)}{dt} = -K_2 n_{F_2}(t) n_H(t)\,, \qquad \text{(A5)}$$

where $K_2 = 4\pi D R_2 \equiv \kappa K$, and $\kappa = R_2/R$ is a ratio of cross-sections for the interstitial recombination with the dimer and single electronic centers. Since the concentration on the righ hand side $n_H(t) = n_0 C(t)$ is known, eq. (A2), one gets

$$d[ln\, n_{F_2}(t)] = -\kappa K n_0 C(t) dt \equiv d[ln\, C^{\kappa}(t)]\,. \qquad \text{(A6)}$$

In other words, the decay of dimer center concentration is related in a simple way to that for that of single defects:

$$\frac{F_2(t)}{F_2(0)} = C^{\kappa}(t)\ . \qquad \text{(A7)}$$

This is why both types of centers decay in the same temperature range.

Now we can consider kinetics of the mutual transformations of three types of the F_2 centers: $F_2(1) \rightarrow F_2(2)$, and $F_2(2) \rightarrow F_2(3)$.

Let us introduce the relative defect concentrations (probabilities) $W_i(t)$, i=1,2,3, with the normalization $W_1(t) + W_2(t) + W_3(t) = 1$ and initial condition $W_i(0) = w_i$. Then the probabilities to find three types of centers are defined by the following set of kinetic equations:

$$\frac{d\, W_1(t)}{dt} = -p_1 W_1(t)\,, \qquad \text{(A8)}$$

$$\frac{d\, W_2(t)}{dt} = p_1 W_1(t) - p_2 W_2(t), \qquad \text{(A9)}$$

$$\frac{d\, W_3(t)}{dt} = p_2 W_2(t), \qquad \text{(A10)}$$

where the transformation rate $p_1 = p_1^0 \exp(-E_b/k_B T)$ corresponds to the process $F_2(1) \rightarrow F_2(2)$, and then the rate $p_2 = p_2^0 \exp(-E_c/k_B T)$ to the process $F_2(2) \rightarrow F_2(3)$. These equations were numerically solved, provided the constant heating rate $\beta = \frac{d}{dt} T(t) = const$. Using the least square method, we obtained the main kinetic parameters – activation energies for mutual transformations E_b and E_c, two pre-exponents $P_1 = p_1^0/\beta$

and $P_2=p_2^0/\beta$, recombination parameter κ and initial defect populations w_i. The obtained results are discussed in Section 3.2.

References

1. B.D. Evans, A review of the optical properties of anion lattice vacancies, and electrical conduction in α-Al_2O_3: their relation to radiation-induced electrical degradation. J. Nucl. Mater. **219** (1995) 202-223 (review article).
2. J. Valbis, N. Itoh, Electronic excitations, luminescence and lattice defect formation in α-Al_2O_3 crystals. Radiat. Eff. Defects Solids **116** (1991) 171–189.
3. R. Vila, A. Ibarra, M. de Castro, F.W. Clinard, Thermally stimulated depolarization currents in neutron-irradiated Al_2O_3. Solid St. Comm. **79** (1991) 295-297.
4. F. Mota, C.J. Ortiz, R. Vila, N. Casal, A. Garcia, A. Ibarra, Calculation of damage function of Al_2O_3 in irradiation facilities for fusion reactor applications. J. Nucl. Mater. **442** (Suppl. 1) (2013) 5699-5704.
5. E. Feldbach, E. Tõldsepp, M. Kirm, A. Lushchik, K. Mizohata, J. Räisänen, Radiation resistance diagnostics of wide-gap optical materials. Optical Materials **55** (2016) 164-167.
6. E.H. Farnum, F.W. Clinard Jr., Electrical properties of Al_2O_3 during irradiation with spallation neutrons. J. Nucl. Mater. **219** (1995), 161-164.
7. T. Shikama, S. J. Zinkle. Long term degradation of electrical insulation of Al_2O_3 under high flux fission reactor irradiation. J. Nucl. Mater. **258–263** (1998) 1861-1866.
8. V.A. Skuratov, V.A. Altynov, S.M. Abu AlAzm. Luminescence characterization of radiation damage of α-Al_2O_3 under 1 MeV/amu ion irradiation. J. Nucl. Mater. **233–237** (1996) 1321-1324.
9. E.A. Kotomin, A.I. Popov, Radiation-induced point defects in simple oxides. Nucl. Instrum. Meth. Phys. Res. B **141** (1998) 1-15 (a review article)
10. A.M. Stoneham, Theory of Defects in Solids, Oxford, 1975; N. Itoh and A.M. Stoneham, *Material Modification by Electronic Excitations,* Oxford, 2001.
11. A.I. Popov, E.A. Kotomin, J. Maier, Basic properties of the F-type centers in halides, oxides and perovskites. Nucl. Instrum. Meth. Phys. Res. ***268*** (2010). 3084-3089.
12. A. Lushchik, Ch. Lushchik, K. Schwartz, F. Savikhin, E. Shablonin, A. Shugai, E. Vasil'chenko, Creation and clustering of Frenkel defects at high density of electronic excitations in wide-gap materials. Nucl. Instrum. Meth. B **277** (2012) 40-44.
13. A. Lushchik, Ch. Lushchik, K. Schwartz, E. Vasil'chenko, T. Kärner, I. Kudryavtseva, V. Issakhanyan, A. Shugai, Stabilization and annealing of

interstitials formed by radiation in binary metal oxides and fluorides. Nucl. Instrum. Meth. Phys. Res. B **266** (2008) 2868–2871.

14. E.A. Kotomin, A.I. Popov, R.I. Eglitis, Correlated annealing of radiation defects in alkali halide crystals. Journal of Physics: Condensed Matter **4** (1992) 5901.
15. A.C. Lushchik, A.G. Frorip, Thermalized and hot interstitial halogen ions in alkali halides. Phys. Stat. Sol. (b) **161** (1990) 525-535.
16. M.A. Monge, A.I. Popov, C. Ballesteros, R. González, Y. Chen, E.A. Kotomin, Formation of anion vacancy cluster and nano cavities in thermochemically reduced MgO single crystals. Phys. Rev. B **62** (2000) 9299-9304.
17. A.I. Popov, M.A. Monge, R. González, Y. Chen, E.A. Kotomin, Dynamics of *F*-center annihilation in thermochemically reduced MgO single crystals. Solid State Commun. **118** (2001) 163-167.
18. E.A. Kotomin, A.I. Popov, In: Radiation Effects in Solids, NATO Science Series II-Mathematics Physics and Chemistry (E. Kotomin, K.Sikafus eds.), **235** (2007) 153–192
19. K.H. Lee, J.H. Crawford Jr, Additive coloration of sapphire. Applied Physics Letters **33** (1978) 273-275.
20. B. Savoini, D. Caceres, I. Vergara, R. Gonzalez, J.M. Santiuste, Radiation damage in neutron-irradiated yttria-stabilized-zirconia single crystals. J. Nucl. Mater. **277** (2000) 199-203.
21. A.V. Kruzhalov, S.V. Gorbunov, B.V. Shulgin, V.A. Maslov, Pis'ma Zhurnal Technicheskoi Fiziki **10** (1984) 1503.
22. K. Atobe, N. Ishimoto, and M. Nakagawa, Irradiation-Induced Aggregate Centers in Single Crystal $A1_2O_3$. Phys. Stat. Sol. (a), **89** (1985) 155.
23. M. Izerrouken and T. Benyahia, Absorption and photoluminescence study of Al_2O_3 single crystal irradiated with fast neutrons. Nucl. Instrum. Meth. Phys. Res. B **268** (2010) 2987–2990.
24. S. Ikeda, T. Uchino, Temperature and Excitation Energy Dependence of the Photoionization of the F_2 Center in α-Al_2O_3. J. Phys. Chem. C **118** (2014) 4346–4353.
25. B.D. Evans, M. Stapelbroek, Optical Vibronic Absorption Spectra in 14.8 MeV Neutron Damaged Sapphire. Solid State Commun. **33** (1980) 765−770.
26. G.J. Pogatshnik, Y. Chen, B.D. Evans, A Model of Lattice Defects in Sapphire. IEEE Trans. Nucl. Sci., **NS-34** (1987) 1709−1712.
27. M. Itou, A. Fujiwara, T. Uchino, Reversible Potoinduced Interconversion of Color Centers in α-Al_2O_3 Prepared under Vacuum. J. Phys. Chem. C **113** (2009) 20949−20957.
28. V.N. Kuzovkov, E.A.Kotomin, A.I. Popov, Kinetics of dimer F_2 type center annealing in MgF_2 crystals. Nucl. Instrum. Meth. Phys. Res. B, 2018, in press, http://dx.doi.org/10.1016/j.nimb.2017.10.025
29. V. Baryshnicov, T. Kolesnikova, E. Martynovich, L. Schepina. Mechanisms of transformation and restruction of color centers in single α-Al_2O_3 crystals. Solid State Physics, **32** (1990) 291.

30. V.S. Kortov, V.A. Pustovarov, S.V. Zvonarev, T.V. Shtang, Luminescence and radiation-induced color centers in anion-deficient alumina crystals after high-dose irradiation. Rad. Measur. **90** (2016) 90-93.
31. M. Okada, T. Seiyama, C. Ichihara, M. Nakagawa, Optical properties of MgO irradiated by fast neutrons. J. Nucl. Mater. **133–134** (1985) 745-748.
32. D.O. O'Connell, B. Henderson, J.M. Bolton, Uniaxial stress and polarisation studies of F_2 centre luminescence in MgO. Solid State Commun. **38** (1981) 283-285.
33. J.D. Bolton, B. Henderson, D.O. O'Connell, Photoluminescence of F^{2+}_2 centres in additively coloured magnesium oxide. Solid State **38** (1981) 287-290.
34. Y. Uenaka, T. Uchino, Photoexcitation, trapping, and recombination processes of the F-type centers in lasing MgO microcrystals. Phys. Rev. B **83** (2011) 195108.
35. K. Uchida, K. Noda, T. Tanifuji, S. Nasu, T. Kirihara, A. Kikuchi, Optical absorption spectra of neutron□irradiated Li_2O. Phys. Stat. Sol. (a) **58** (1980) 557-566.
36. D.J. Gravesteijn, M. Glasbeek, Optically detected magnetic resonance and spin coherence in the phosphorescent state of exchange-coupled F^+-center pairs in CaO. Phys. Rev. B **19** (1979) 5549.
37. M.A. Monge, R. Gonzalez, J.E. Santiuste, R. Pareja, Y. Chen, E.A. Kotomin, A.I. Popov, Photoconversion and dynamic hole recycling process in anion vacancies in neutron-irradiated MgO crystals. Phys. Rev. B **60** (1999) 3787.
38. M.A. Monge, R. Gonzalez, J.E. Santiuste, R. Pareja, Y. Chen, E.A. Kotomin, A.I. Popov, Photoconversion of F^+ centers in neutron-irradiated MgO. Nucl. Instrum. Meth. Phys. Res. B **166** (2000) 220.
39. R.S. Averback, P. Ehrhart, A.I. Popov, A. von Sambeek, Defects in ion implanted and electron irradiated MgO and Al_2O_3. Radiat. Eff. Defects Solids, **136** (1995) 1079-1083.
40. E.A. Kotomin, A. Stashans, L.N. Kantorovich, A.I. Lifshitz, A.I. Popov, I.A. Tale, J.-L. Calais, Calculations of the geometry and optical properties of F_{Mg} and dimer (F_2 type) centers in corundum crystals. Phys. Rev. B **51** (1995) 8770-8779.
41. E.A. Kotomin, V.N. Kuzovkov, A.I. Popov, and R. Vila, Kinetics of *F* center annealing and colloid formation in Al_2O_3. Nucl. Instr. Meth. Phys. Res. B **374** (2016) 107–110.
42. V.N. Kuzovkov, A.I. Popov, E.A. Kotomin, A.M. Moskina, E. Vasil'chenko, and A. Lushchik, Theoretical analysis of the kinetics of low-temperature defect recombination in alkali halide crystals. Low Temp. Phys. **42** (2016) 748-755.
43. R. Ramírez, M. Tardío, R. González, J.E. Muñoz Santiuste, M.R. Kokta. Optical properties of vacancies in thermochemically reduced Mg-doped sapphire single crystals. J. Appl. Phys. 101 (2007) 123520 (1-12).
44. B.G. Draeger, G.P. Summers, Defects in unirradiated α-Al_2O_3, Phys. Rev. B **19** (1979) 1172-1177.
45. J. M. Bunch, F. W. Clinard JR. Damage of Single-Crystal Al_2O_3 by 14-MeV Neutrons. Journal of The American Ceramic Society **57** (1974) 279-280.

46. M. Izerrouken, Y. Djouadi, H. Zirour. Annealing process of F- and F+-centers in Al_2O_3 single crystal induced by fast neutrons irradiation. Nucl. Instrum. Meth. Phys. Res. B **319** (2014) 29–33.
47. C.Grygiel, F. Moisy, M. Sall, H. Lebius, E. Balanzat, T. Madi, T. Been, D. Marie, I. Monnet. In situ kinetics of modifications induced by swift heavy ions in Al_2O_3: color center formation, structural modification and amorphization. Acta Materialia **140** (2017) 157-167.
48. V.N. Kuzovkov, E.A. Kotomin, A.I. Popov, J. Maier, R. Vila, Anomalous kinetics of diffusion-controlled defect annealing in irradiated ionic solids. J. Phys. Chem. A **122** (2018) 28-32 .
49. A. Platonenko, D. Gryaznov, Yu.F. Zhukovskii, E.A. Kotomin, *Ab initio* simulations on charged interstitial oxygen migration in corundum. Nucl. Instrum. Meth. Phys. Res. B (2018), in press https://doi.org/10.1016/j.nimb.2017.12.022
50. Yu.F. Zhukovskii, A. Platonenko, S. Piskunov, E.A. Kotomin, *Ab initio* simulations on migration paths of interstitial oxygen in corundum. Nucl. Instrum. Meth. Phys. Res. B **374** (2016) 29-34.
51. B.D. Evans, Optical properties of lattice defects in α-Al_2O_3. Nucl. Instr. and Meth. B **91** (1994) 258-262.
52. G. Zvejnieks and V.N. Kuzovkov, Monte-Carlo simulations for Lotka-type model with reactant surface diffusion and interactions. Phys. Rev. E **63** (2001) 051104.
53. P.K. Jha, V.N. Kuzovkov, B.A. Grzybowski, and M. Olvera de la Cruz, Dynamic self-assembly of photo-switchable nanoparticles. Soft Matter **8** (2012) 227–234.
54. A.S. El-Said, R. Neumann, K. Schwartz, C. Trautmann, Swelling and creation of color centers in MgF_2 single crystals irradiated with energetic heavy ions. Nucl. Instrum. Meth. Phys. Res. B **245** (2006) 250–254.
55. B.D.Evans, M.Stapelbroeck, Optical properties of the F+ center in crystalline Al_2O_3. Phys. Rev. B 1**8** (1978) 7089.
56. B.D. Evans, G.J. Pogatshnik, Y. Chen, Optical properties of lattice defects in $\alpha-Al_2O_3$. Nucl. Instrum. Methods B, **91** (1994) 258-262.
57. E.A. Kotomin, A.I. Popov, A. Stashans, Computer modeling of radiation damage in cation sublattice of corundum. Phys. Stat. Sol. B **207** (1998) 69-73.
58. M.V. Smoluchowski, Versuch einer mathematischen Theorie der Koagulationskinetik kolloider Lo̸sungen. Z. Phys. Chem. B **92** (1917) 129-168.
59. V.N. Kuzovkov and E.A. Kotomin, Kinetics of bimolecular reactions in condensed media: critical phenomena and microscopic self-organisation. Rep. Prog. Phys. **51** (1988) 1480-1524.
60. E.A. Kotomin and V.N. Kuzovkov, Phenomenological kinetics of Frenkel defect recombination and accumulation in ionic solids. Rep. Prog. Phys. **55** (1992) 2079-2188.
61. E.A. Kotomin and V.N. Kuzovkov, *Modern aspects of diffusion-controlled reactions.* vol. **34** in a series of Comprehensive Chemical Kinetics (Amsterdam: Elsevier, 1996).